Supporting Information for:

Multicopper Models for the Laccase Active Site: Effect of Nuclearity on Electrocatalytic Oxygen Reduction

Edmund C. M. Tse, David Schilter, Danielle L. Gray, Thomas B. Rauchfuss and Andrew A. Gewirth*

Department of Chemistry

University of Illinois at Urbana-Champaign

600 S. Mathews Avenue

Urbana, IL 61801

*author to whom correspondence should be addressed:

Tel: 217-333-8329, Fax: 217-244-3186, email: agewirth@illinois.edu

List of Figures

List of Tables

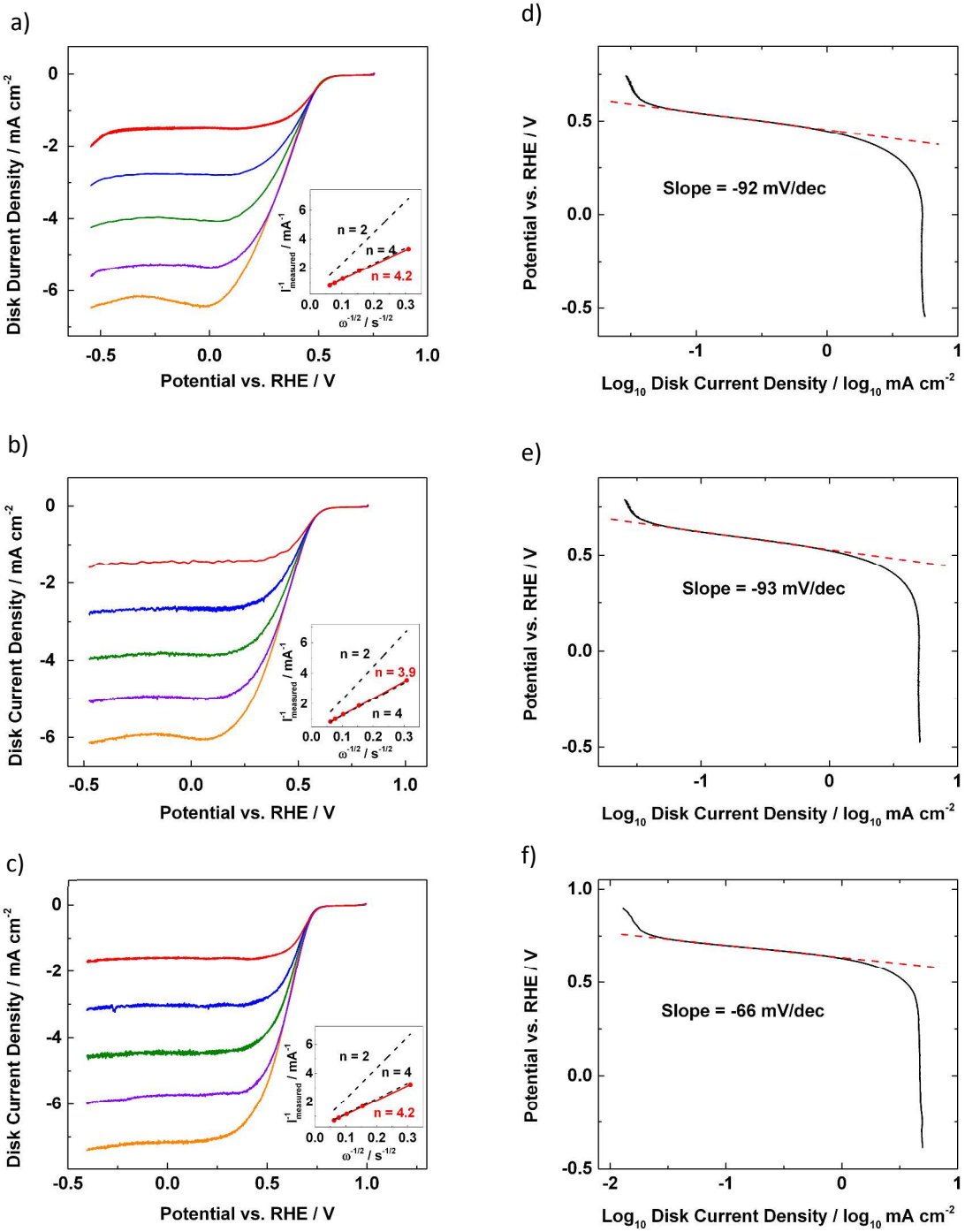

Fig. S1. RDE voltammograms and Koutecky-Levich plots (inset) of $[Cu(\mathbf{1})]^{2+}$ supported on Vulcan XC-72 in (a) pH 4, (b) pH 7, and (c) pH 10 O_2-saturated Britton-Robinson buffer solutions with a scan rate of 10 mV/s at 100 (red), 400 (blue), 900 (green), 1600 (violet), and 2500 rpm (orange). Tafel plots $[Cu(\mathbf{1})]^{2+}$ supported on Vulcan XC-72 in (d) pH 4, (e) pH 7, and (f) pH 10 O_2-saturated Britton-Robinson buffer solutions (10 mV/s, 1600 rpm).

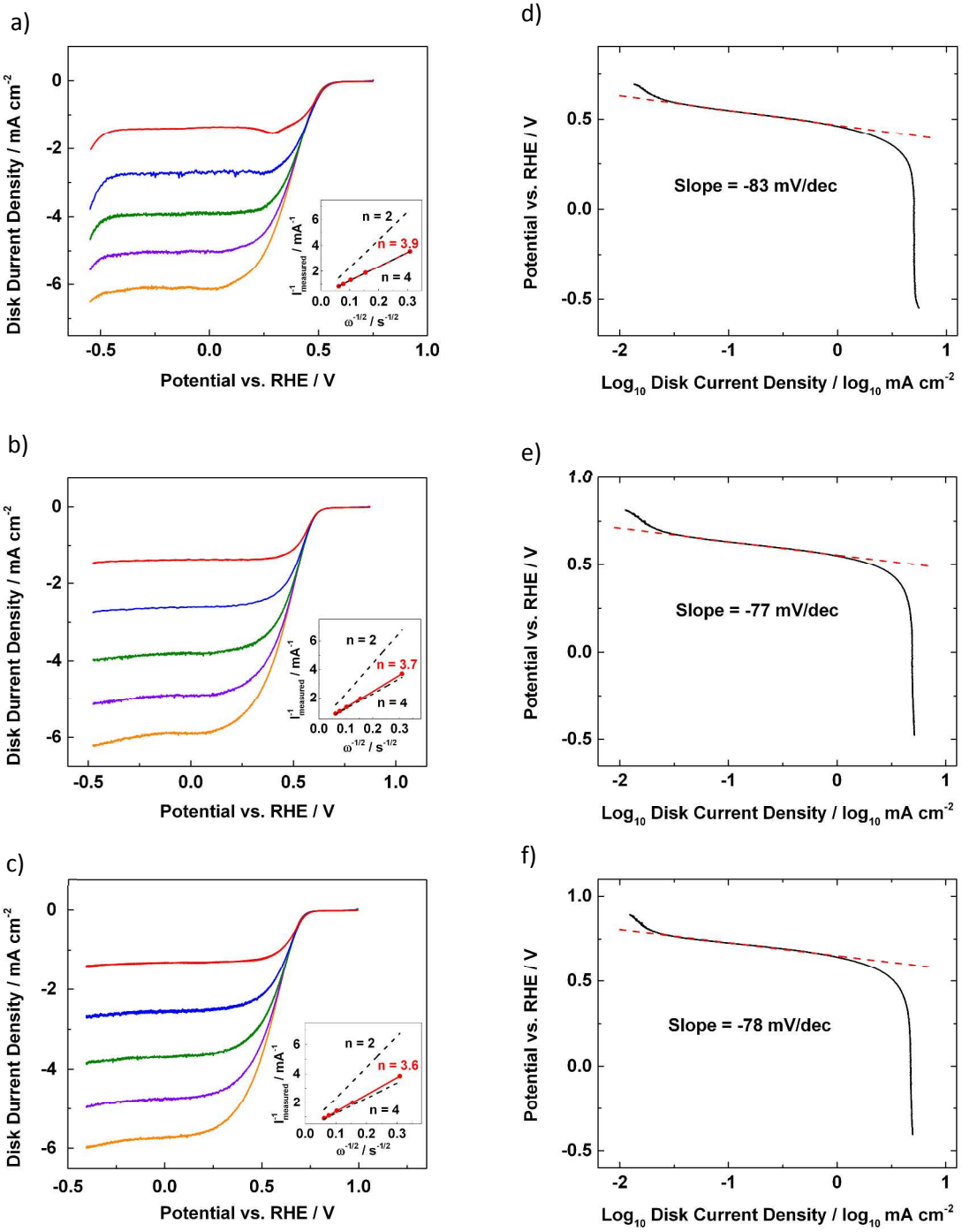

Fig. S2. RDE voltammograms and Koutecky-Levich plots (inset) of $[Cu_2(\mathbf{2})]^{4+}$ supported on Vulcan XC-72 in (a) pH 4, (b) pH 7, and (c) pH 10 O_2-saturated Britton-Robinson buffer solutions with a scan rate of 10 mV/s at 100 (red), 400 (blue), 900 (green), 1600 (violet), and 2500 rpm (orange). Tafel plots of $[Cu_2(\mathbf{2})]^{4+}$ on Vulcan XC-72 in (d) pH 4, (e) pH 7, and (f) pH 10 O_2-saturated Britton-Robinson buffer solutions (10 mV/s, 1600 rpm).

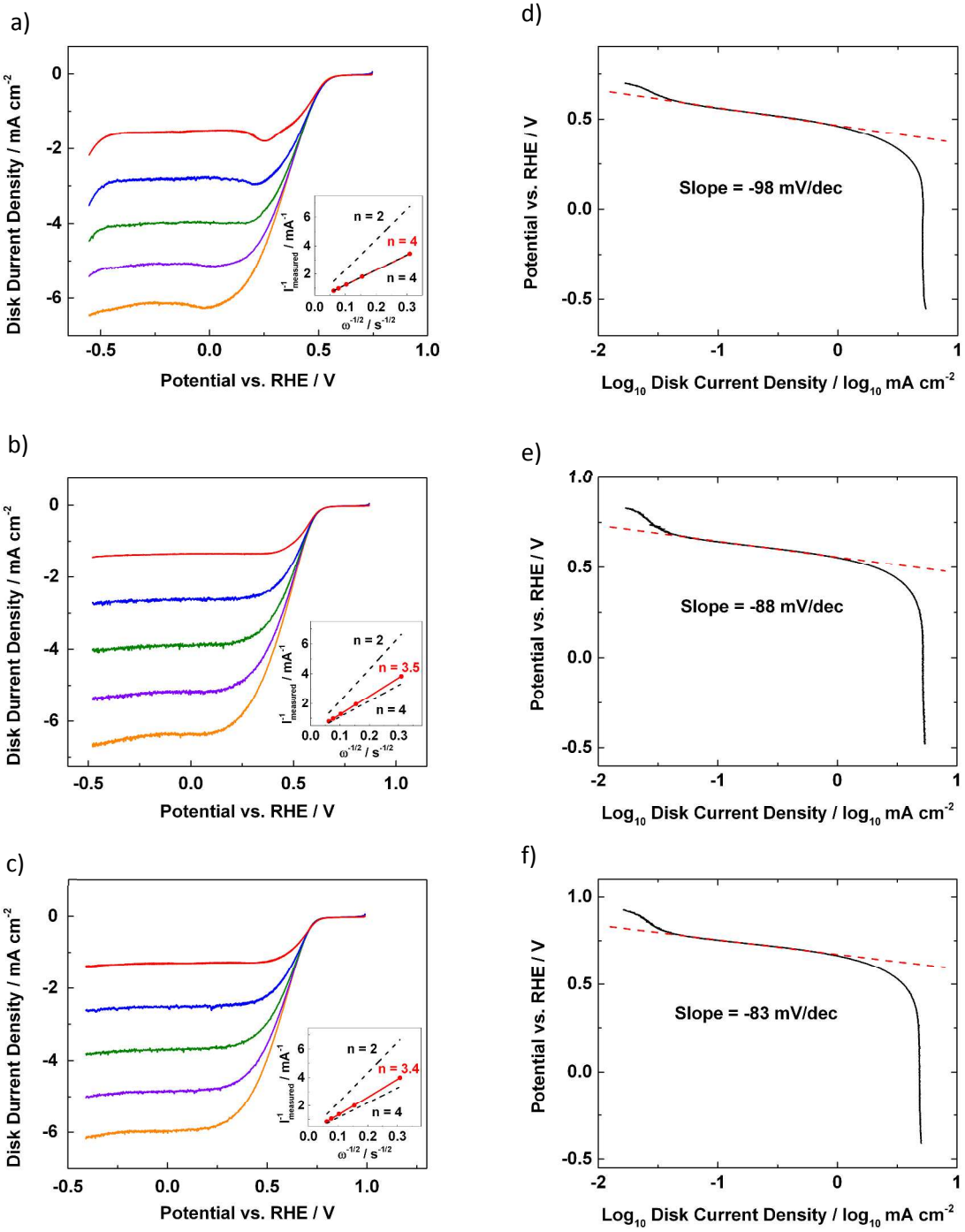

Fig. S3. RDE voltammograms and Koutecky-Levich plots (inset) of $[Cu_2(\mathbf{3})]^{4+}$ supported on Vulcan XC-72 in (a) pH 4, (b) pH 7, and (c) pH 10 O_2-saturated Britton-Robinson buffer solutions with a scan rate of 10 mV/s at 100 (red), 400 (blue), 900 (green), 1600 (violet), and 2500 rpm (orange). Tafel plots of $[Cu_2(\mathbf{3})]^{4+}$ supported on Vulcan XC-72 in (d) pH 4, (e) pH 7, and (f) pH 10 O_2-saturated Britton-Robinson buffer solutions (10 mV/s, 1600 rpm).

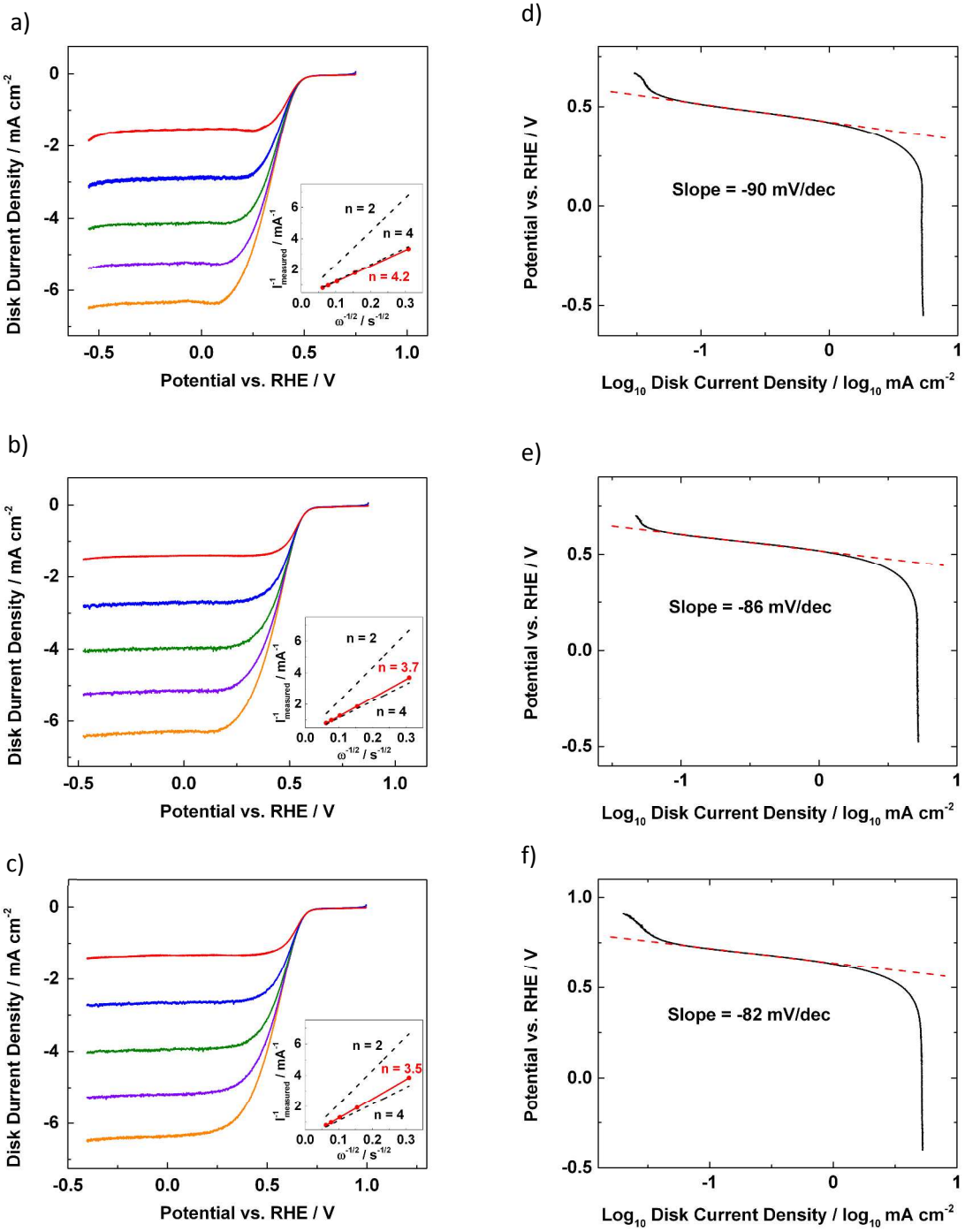

Fig. S4. RDE voltammograms and Koutecky-Levich plots (inset) of $[Cu_3(\mathbf{4})]^{6+}$ supported on Vulcan XC-72 in (a) pH 4, (b) pH 7, and (c) pH 10 O_2-saturated Britton-Robinson buffer solutions with a scan rate of 10 mV/s at 100 (red), 400 (blue), 900 (green), 1600 (violet), and 2500 rpm (orange). Tafel plots of $[Cu_3(\mathbf{4})]^{6+}$ supported on Vulcan XC-72 in (d) pH 4, (e) pH 7, and (f) pH 10 O_2-saturated Britton-Robinson buffer solutions (10 mV/s, 1600 rpm).

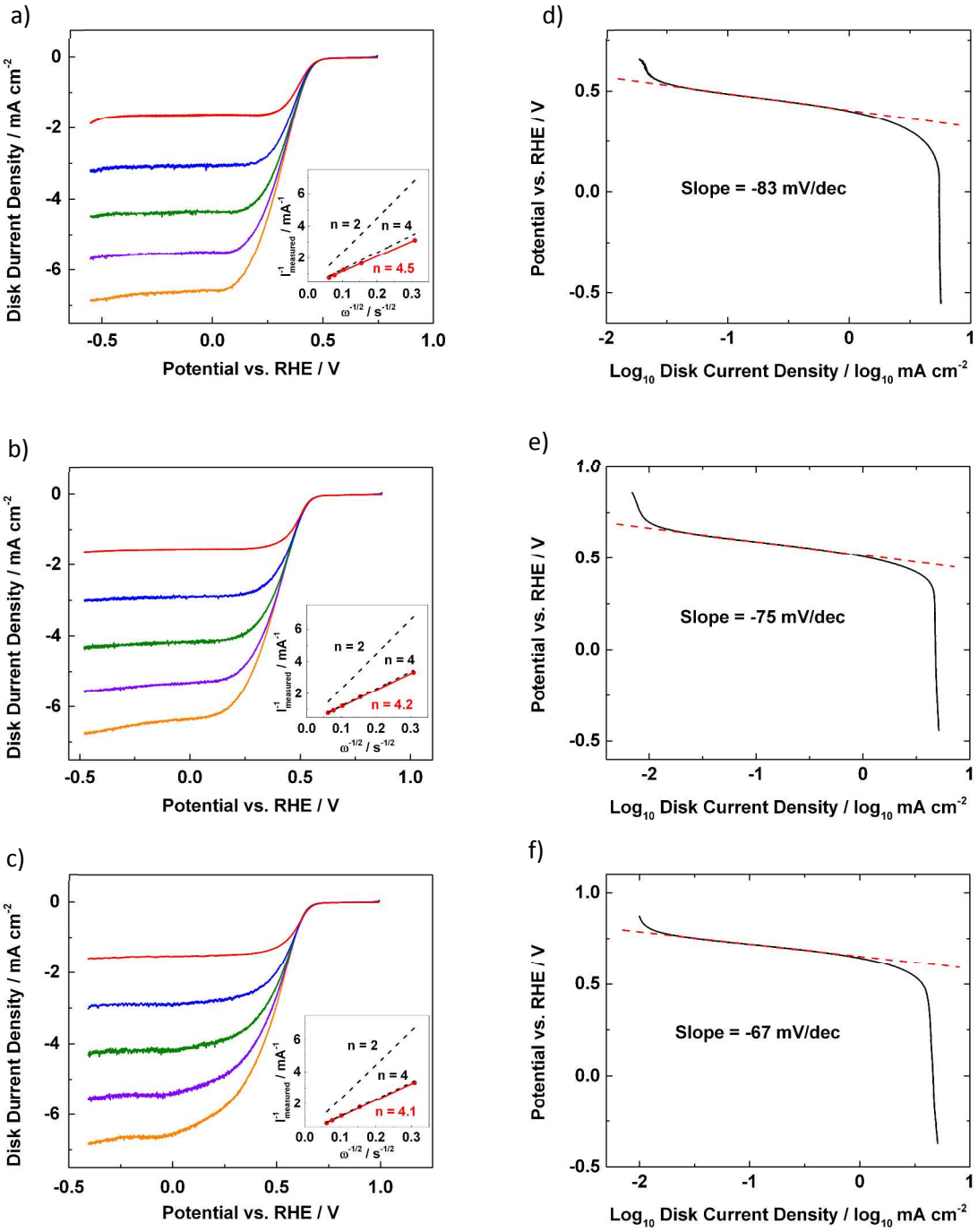

Fig. S5. RDE voltammograms and Koutecky-Levich plots (inset) of $[Cu_3(\mathbf{5})]^{6+}$ supported on Vulcan XC-72 in (a) pH 4, (b) pH 7, and (c) pH 10 O_2-saturated Britton-Robinson buffer solutions with a scan rate of 10 mV/s at 100 (red), 400 (blue), 900 (green), 1600 (violet), and 2500 rpm (orange). Tafel plots of $[Cu_3(\mathbf{5})]^{6+}$ supported on Vulcan XC-72 in (d) pH 4, (e) pH 7, and (f) pH 10 O_2-saturated Britton-Robinson buffer solutions (10 mV/s, 1600 rpm).

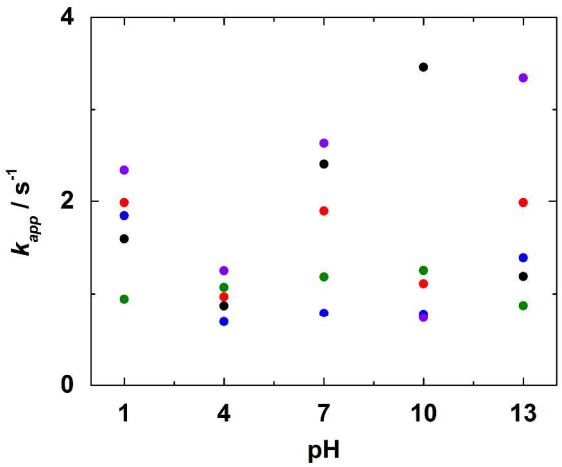

Fig. S6. Apparent electron transfer rate constants (k_{app}) of $[Cu(\mathbf{1})]^{2+}$ (black), $[Cu_2(\mathbf{2})]^{4+}$ (red), $[Cu_2(\mathbf{3})]^{4+}$ (blue), $[Cu_3(\mathbf{4})]^{6+}$ (green), and $[Cu_3(\mathbf{5})]^{6+}$ (purple) vs. pH.

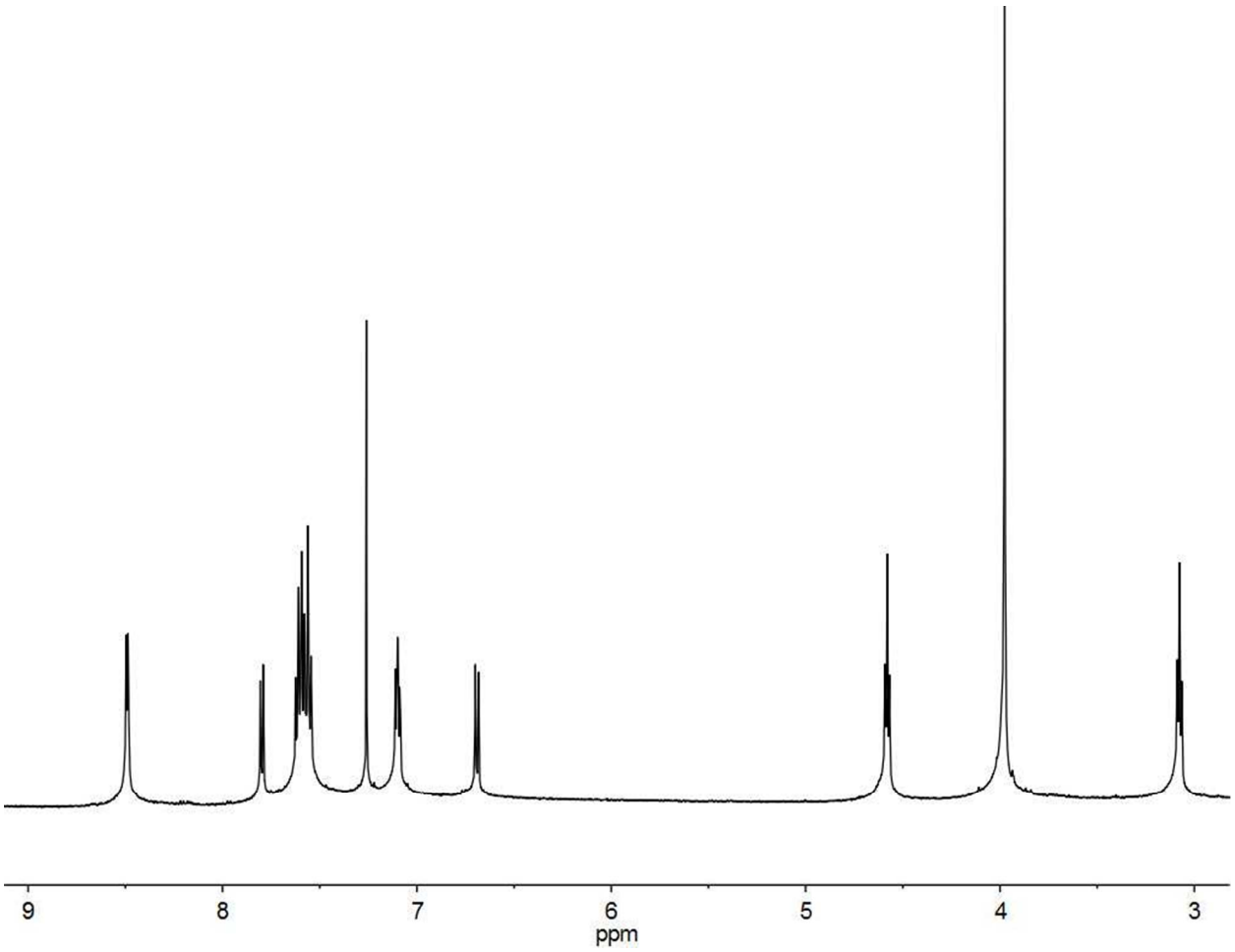

Fig. S7. ^{1}H NMR spectrum of **4** in $CDCl_3$.

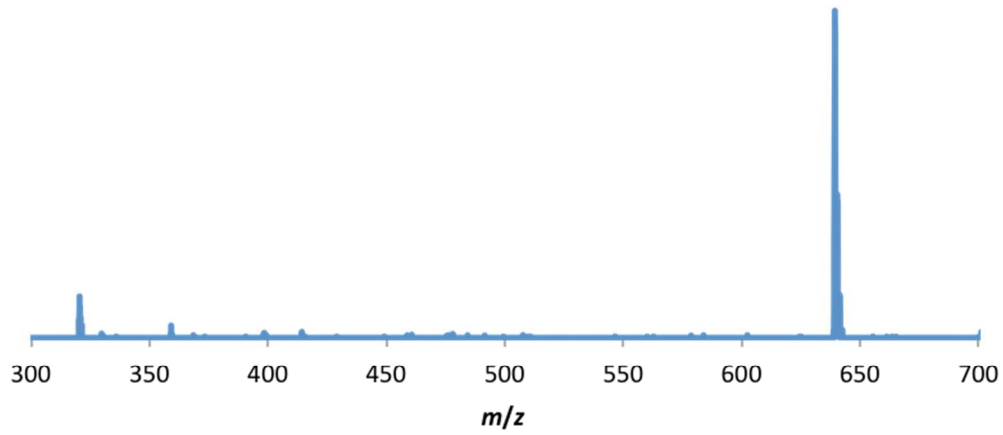

Fig. S8. Positive ion ESI mass spectrum of **4**.

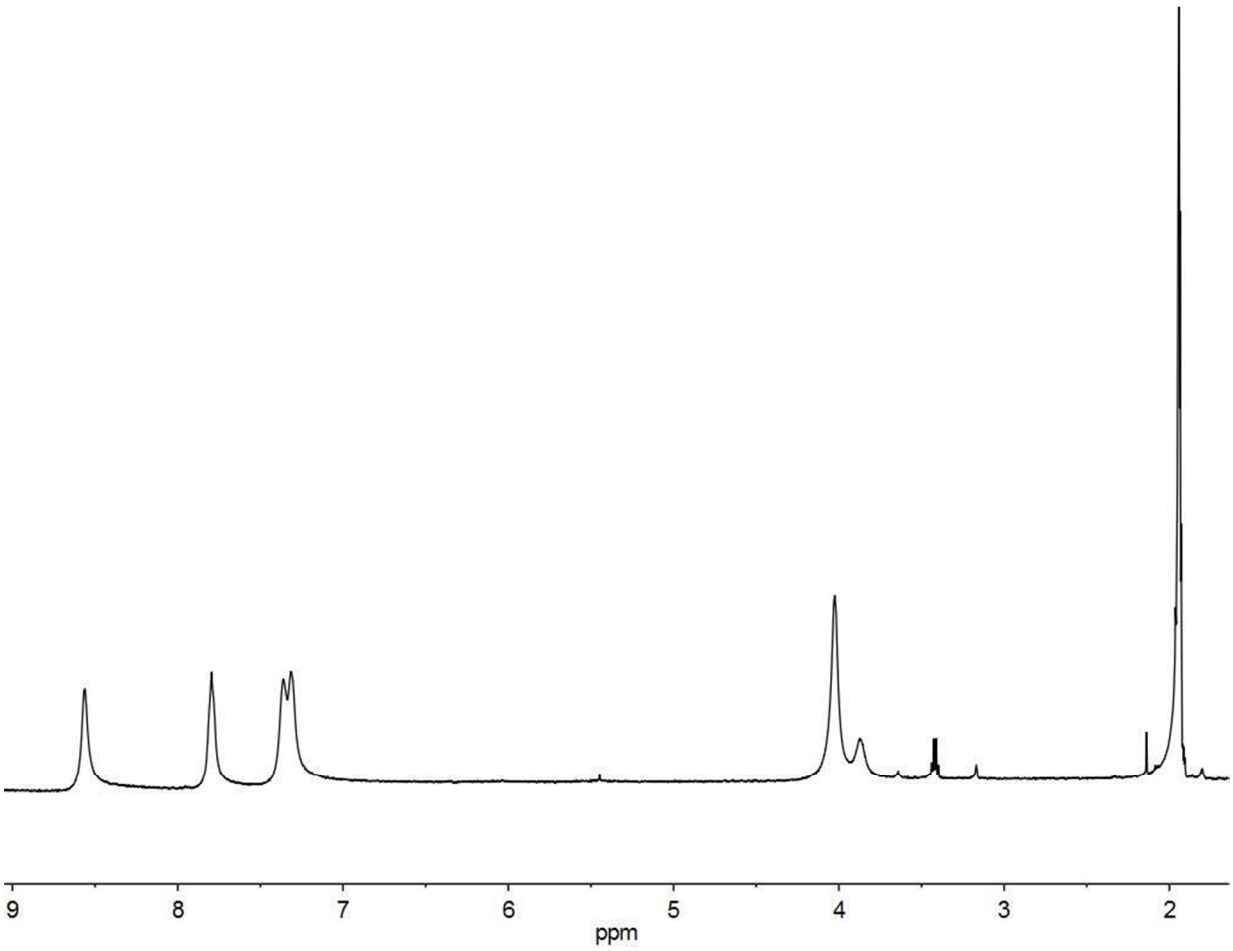

Fig. S9. ^{1}H NMR spectrum of [Cu(MeCN)(**1**)]BF_4 in CD_3CN.

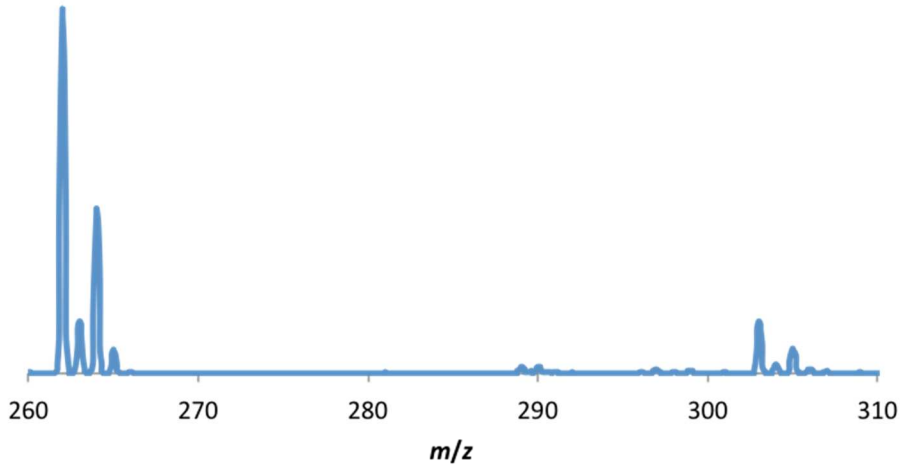

Fig. S10. Positive ion ESI mass spectrum of [Cu(MeCN)(**1**)]BF_4.

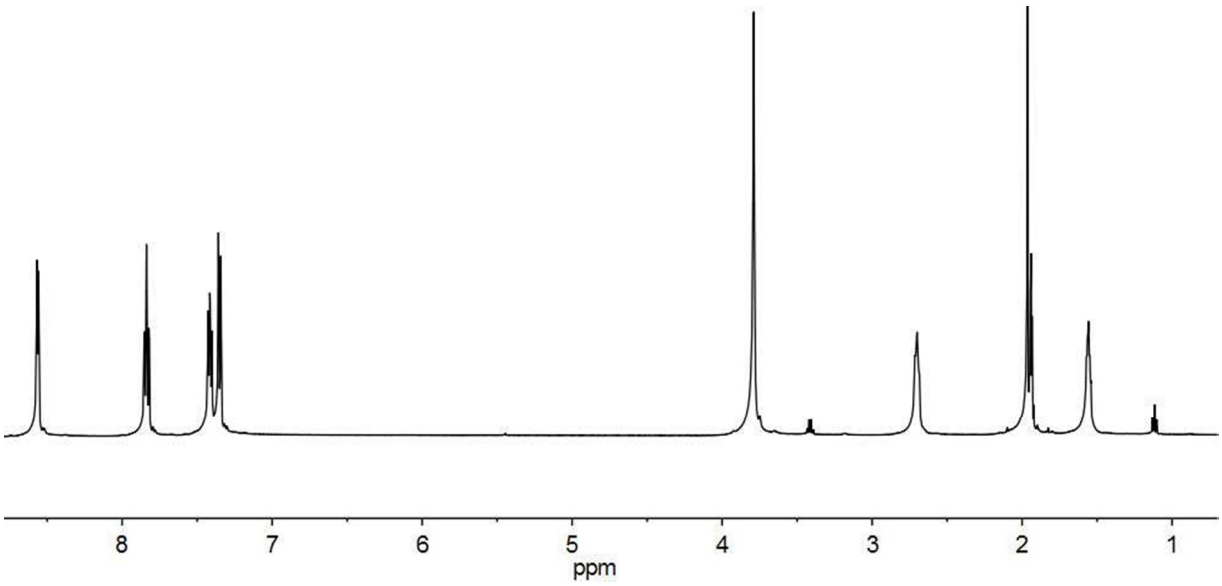

Fig. S11. ^{1}H NMR spectrum of $[Cu_2(MeCN)_2(\mathbf{2})](BF_4)_2$ in CD_3CN. Resonances at 3.42, 1.12 ppm are from residual Et_2O.

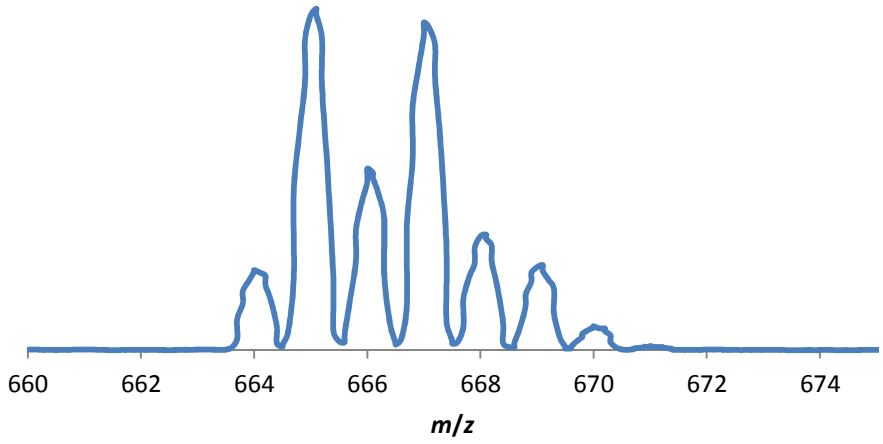

Fig. S12. Positive ion ESI mass spectrum of $[Cu_2(MeCN)_2(\mathbf{2})](BF_4)_2$.

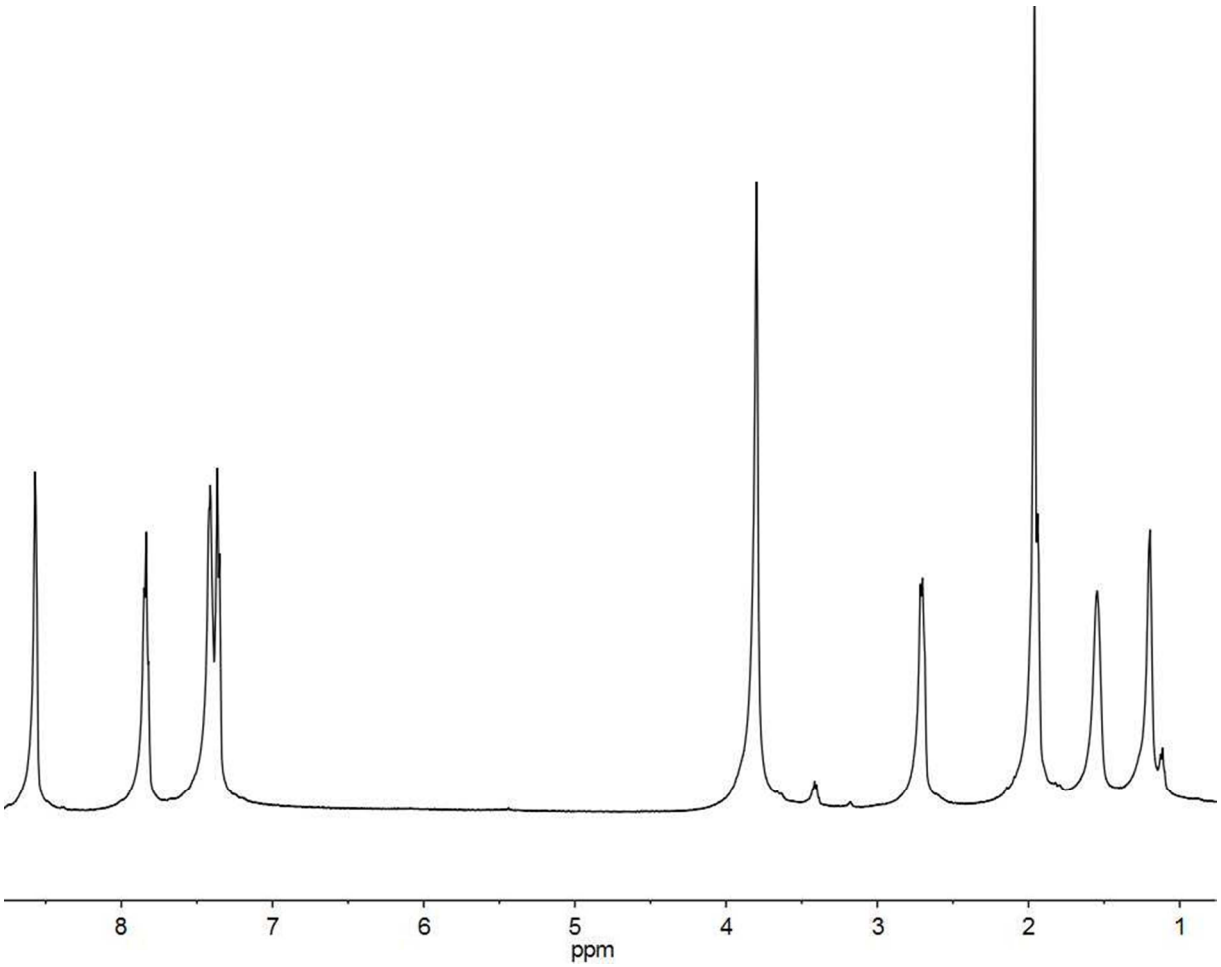

Fig. S13. ^{1}H NMR spectrum of $[Cu_2(MeCN)_2(\mathbf{3})](BF_4)_2$ in CD_3CN. Resonances at 3.42, 1.12 ppm are from residual Et_2O.

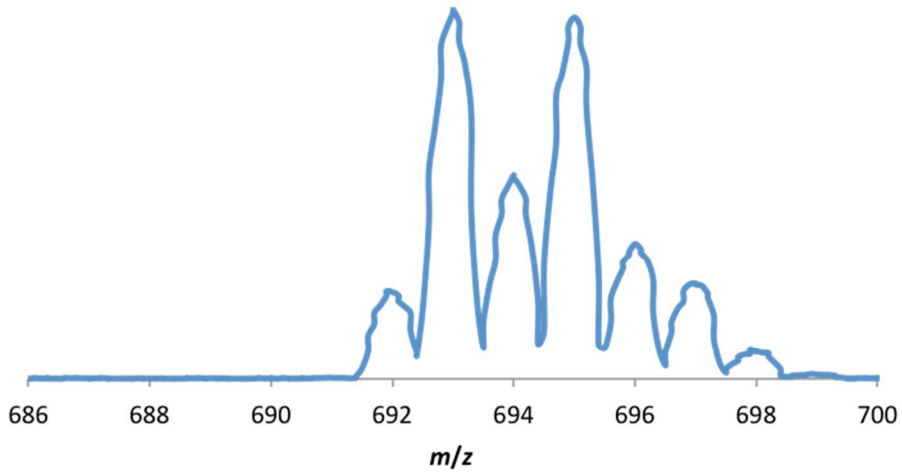

Fig. S14. Positive ion ESI mass spectrum of $[Cu_2(MeCN)_2(\mathbf{3})](BF_4)_2$.

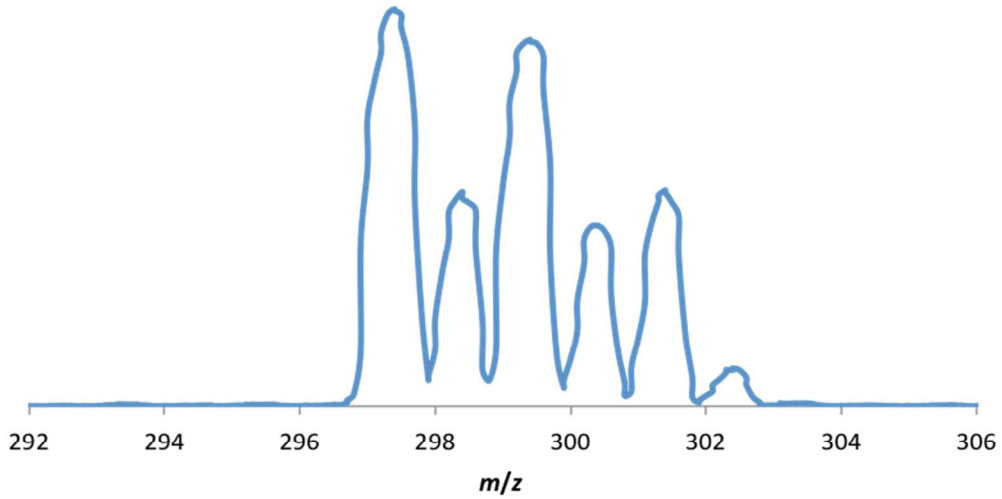

Fig. S15. Positive ion ESI mass spectrum of [$CuCl_2$(**1**)].

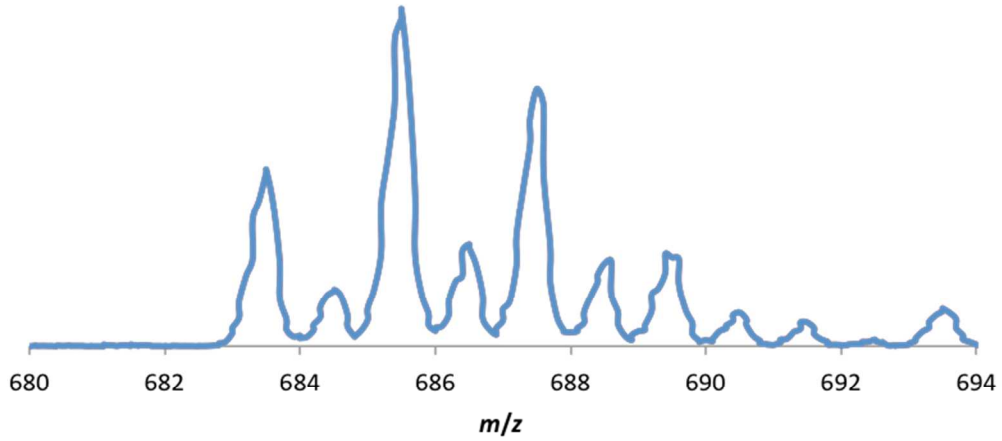

Fig. S16. Positive ion ESI mass spectrum of [Cu_2Cl_4(**2**)].

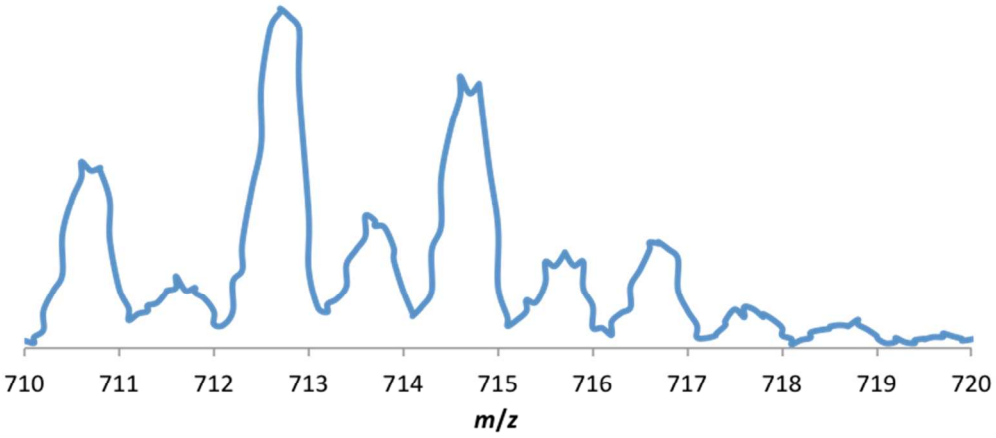

Fig. S17. Positive ion ESI mass spectrum of [Cu_2Cl_4(**3**)].

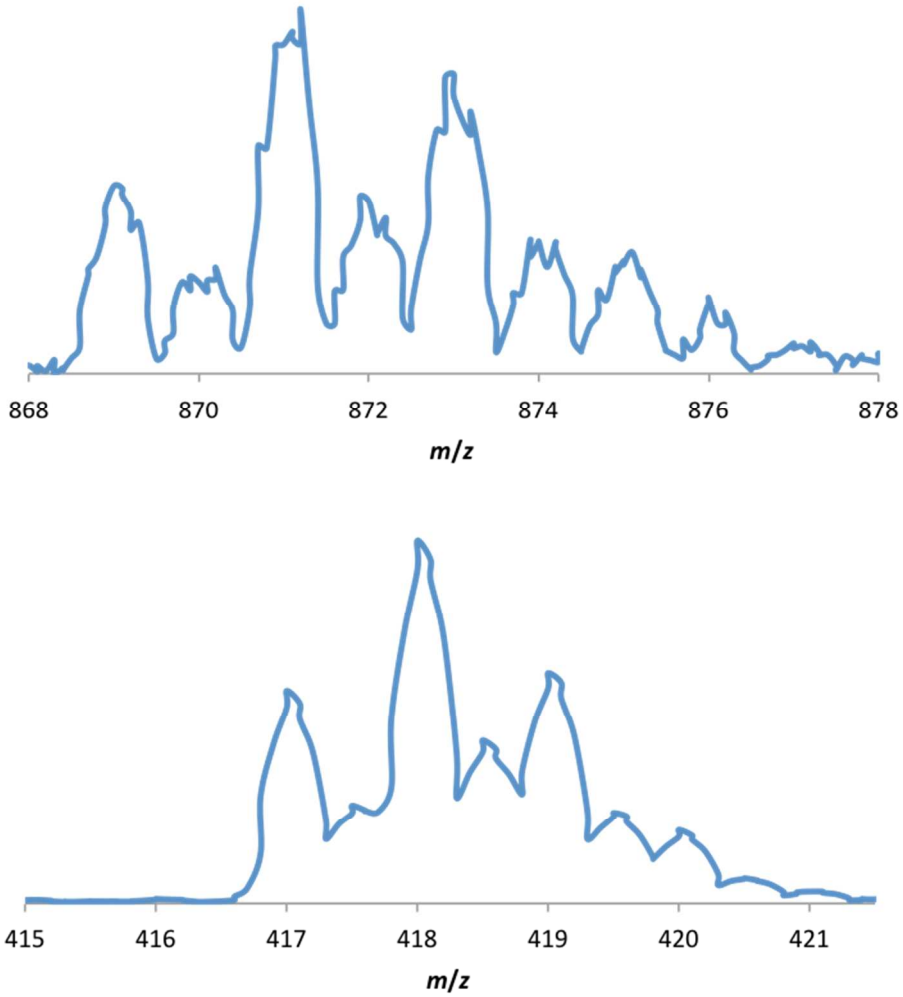

Fig. S18. Partial positive ion ESI mass spectra of [Cu_2Cl_4(**4**)].

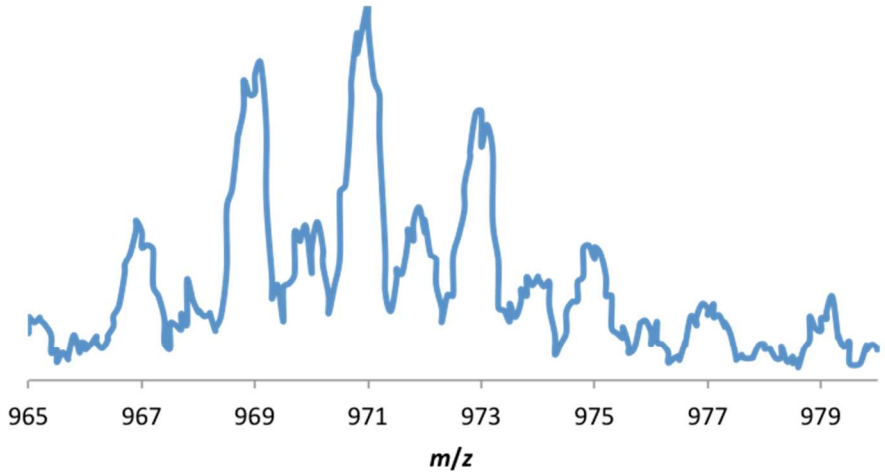

Fig. S19. Positive ion ESI mass spectrum of [Cu_3Cl_6(**4**)].

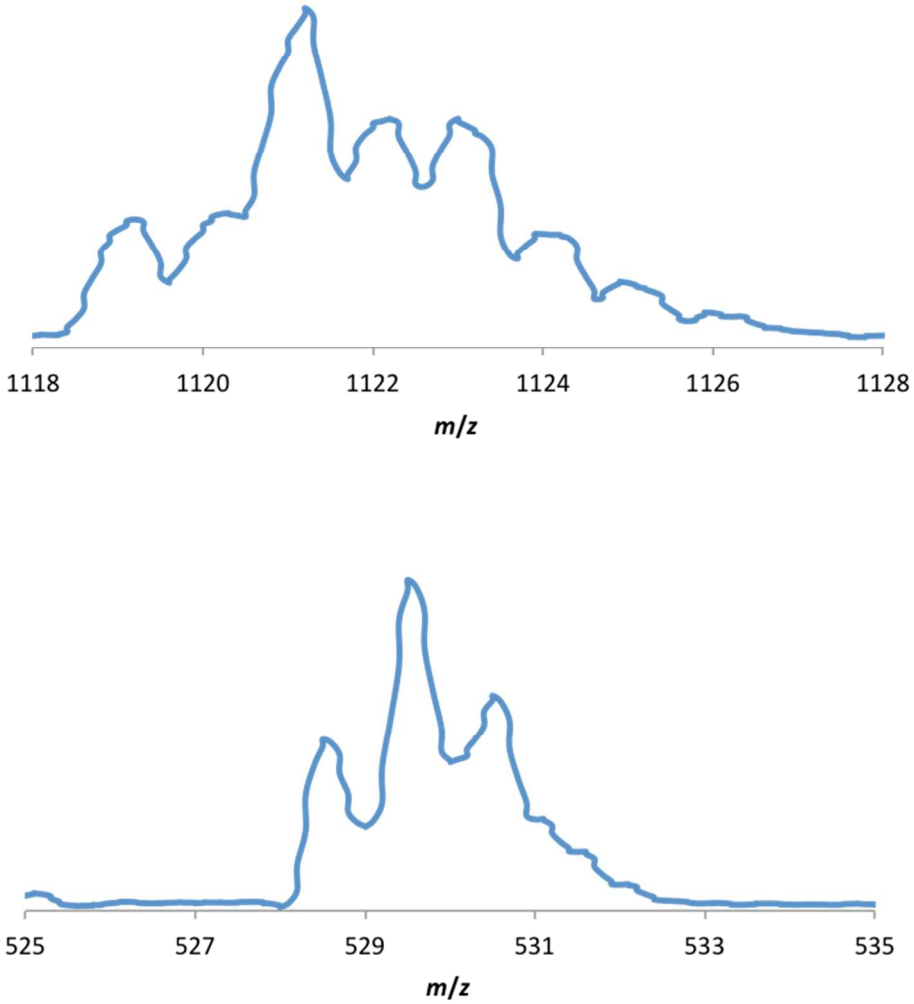

Fig. S20. Partial positive ion ESI mass spectra of $[Cu_2Ag(NO_3)_5(\mathbf{4})]$.

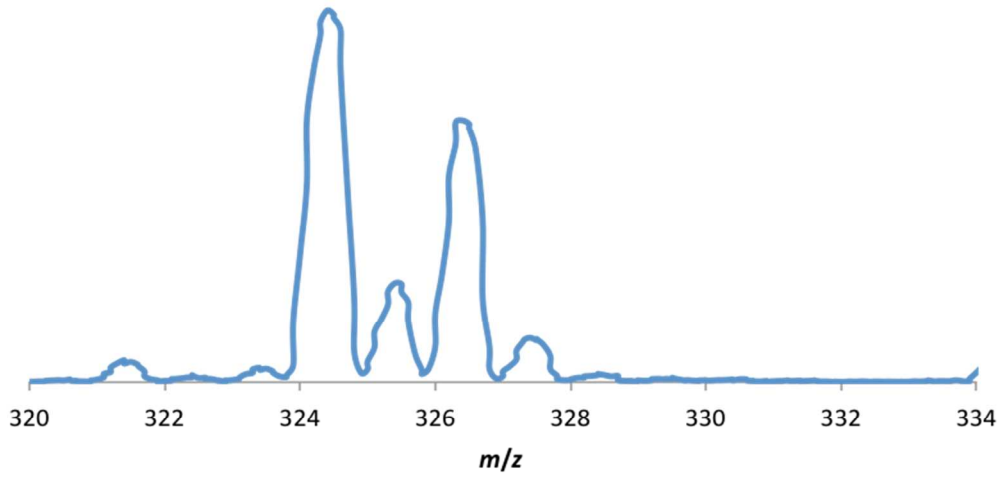

Fig. S21. Positive ion ESI mass spectrum of [$Cu(NO_3)_2$(**1**)].

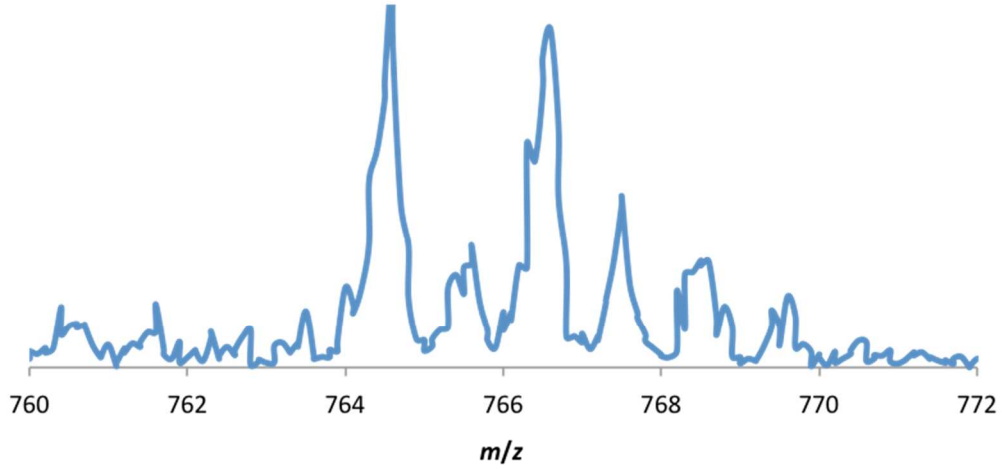

Fig. S22. Positive ion ESI mass spectrum of [$Cu_2(NO_3)_4$(**2**)].

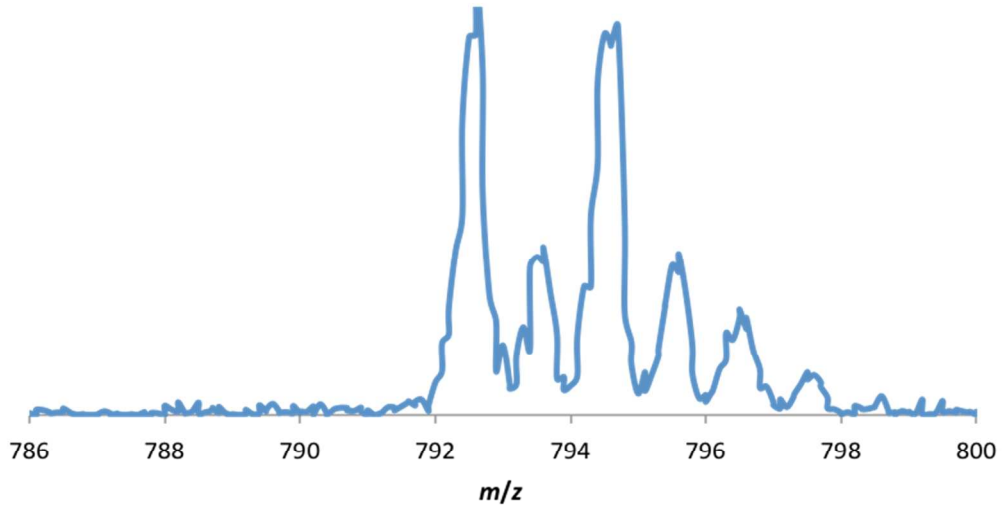

Fig. S23. Positive ion ESI mass spectrum of [$Cu_2(NO_3)_4$(**3**)].

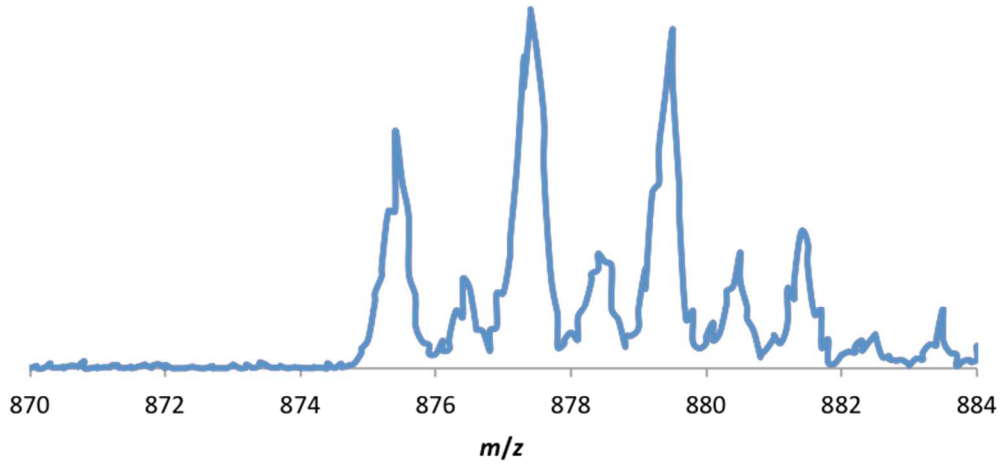

Fig. S24. Positive ion ESI mass spectrum of [$Cu_2(ClO_4)_4$(**2**)].

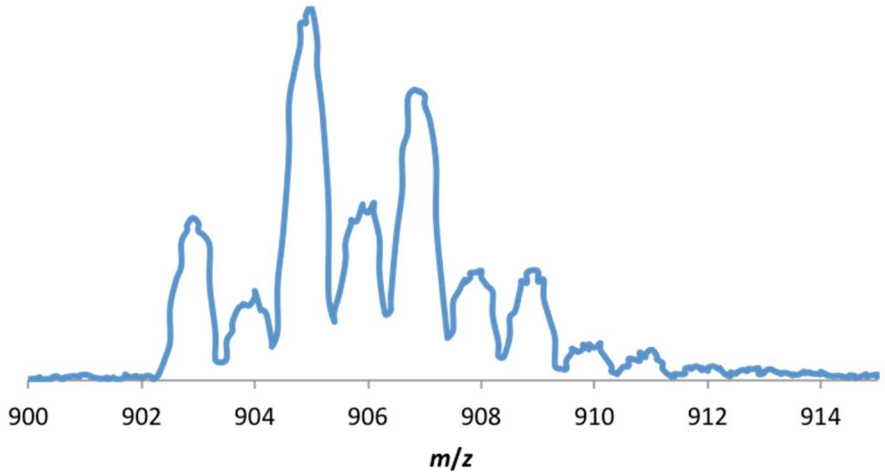

Fig. S25. Positive ion ESI mass spectrum of $[Cu_2(ClO_4)_4(\mathbf{3})]$.

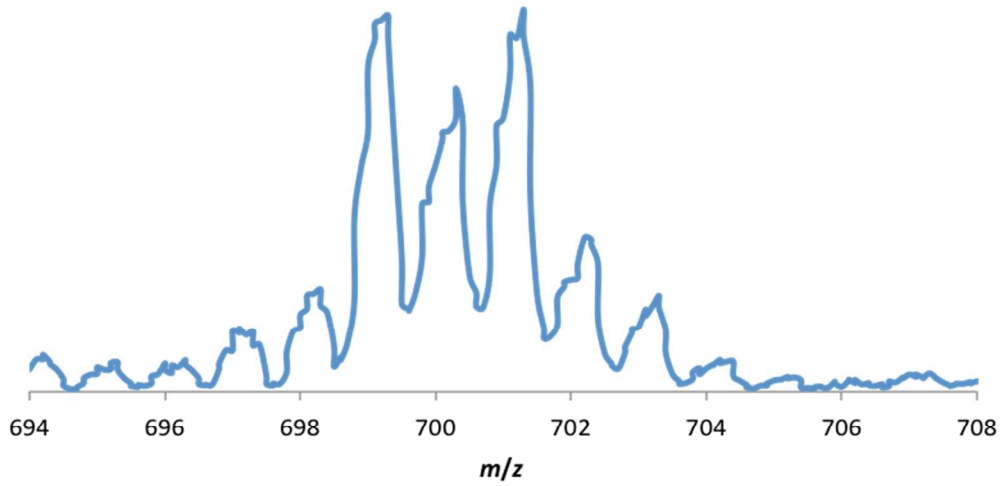

Fig. S26. Positive ion ESI mass spectrum of $[Cu_4(OH)_4(\mathbf{2})_2](BF_4)_4$.

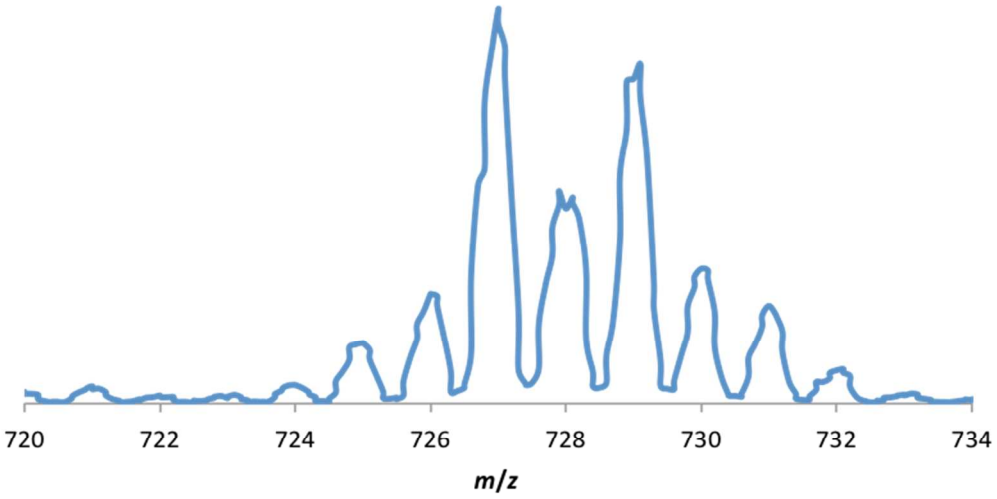

Fig. S27. Positive ion ESI mass spectrum of $[Cu_4(OH)_4(\mathbf{3})_2](BF_4)_4$.

Table S1. Crystal Data and Structure Refinement.

	$[Cu_2Cl_4(\mathbf{3})]\cdot 2H_2O$	$[Cu_4(OH)_4(\mathbf{3})_2](BF_4)_4\cdot 4MeCN\cdot 4H_2O$
formula mass (amu)	813.61	2000.21
space group	P2(1)/c	Pī
Z	2	1
a (Å)	11.361(2)	9.8961(8)
b (Å)	11.795(2)	16.716(1)
c (Å)	14.008(2)	16.885(1)
α (°)	90	62.202(1)
β (°)	105.165(2)	87.664(1)
γ (°)	90	73.505(1)
V (Å^3)	1811.6(5)	2355.2(3)
T (K)	183(2)	168(2)
λ (Å)	0.71073	0.71073
ρ_c (g cm^{-3})	1.492	1.410
μ (cm^{-1})	15.07	9.8
$R(F)^a$	0.0374	0.0431
$R_w(F^2)^b$	0.1094	0.1257

[a] $R(F) = \Sigma||F_o| - |F_c||/\Sigma|F_o|$ for $F_o^2 > 2\sigma(F_o^2)$.
[b] $R_w(F_o^2) = [\Sigma\, w(F_o^2 - F_c^2)^2/\Sigma w F_o^4]$, $w^{-1} = \sigma^2(F_o^2) + (q(F_o^2 + 2F_c^2)/3)^2 + r((F_o^2 + 2F_c^2)/3)$ for $F_o^2 \geq 0$; $w^{-1} = \sigma^2(F_o^2)$ for $F_o^2 < 0$.
For $[Cu_2Cl_4(\mathbf{3})]$, q = 0.0640, r = 0.5623. For $[Cu_4(OH)_4(\mathbf{3})_2](BF_4)_4$, q = 0.0750, r = 0.

Table S2. Hydrogen bond distances (Å) and angles (°) for $[Cu_4(OH)_4(\mathbf{3})_2](BF_4)_4\cdot 4MeCN\cdot 4H_2O$.

D-H...A	d(D-H)	d(H···A)	d(D···A)	<(DHA)
O(2)-H(2)...F(4)	0.83(1)	2.10(2)	2.879(5)	155(4)
O(2)-H(2)...F(4B)	0.83(1)	2.14(2)	2.95(2)	165(4)
O(1)-H(1)...F(3)#2	0.82(1)	2.17(2)	2.960(8)	160(3)
O(1)-H(1)...F(3B)#2	0.82(1)	2.07(2)	2.87(1)	164(3)

Symmetry transformations used to generate equivalent atoms:
#1 -x+1,-y+1,-z #2 x-1,y,z